An Algorithm for Reconstruction of Keck Telescope Segment Figures

KECK ADAPTIVE OPTICS NOTE 468

Christopher Neyman
March 9, 2007

ABSTRACT

This note describes a novel method for the reconstruction of Keck segment figures. The algorithm developed by the C. Roddier and F. Roddier is based on iterative Fourier transforms. The original algorithm was modified to work with the Ultra Fine Screen data from the Keck telescope phasing camera system. The algorithm provides high resolution maps of segment wavefronts suitable for use in AO simulations.

1. Introduction

The wavefront error of individual segments may be a limiting factor in the achievable AO correction for next generation AO systems at Keck Observatory. The optical figure of each segment is measured when it is installed after recoating. The measurements are made with the Ultra Fine Screen (UFS) mode of the Phasing Camera System (PCS). The UFS measurements are a necessary part of segment installation. Each segment is brought to the correct shape by applying forces to a warping harness on the back of each segment. The appropriate forces are determined from UFS measurements of segment optical figures. The UFS mode of the phasing camera system is a Shack-Hartman sensor with optics that zoomed in on a single segment. The UFS system consists of a lenslet array with hexagonal subapertures, 217 of these subapertures are within the boundary of a segment. Only these interior subapertures are used to measure the segment aberrations, see Figure 1.

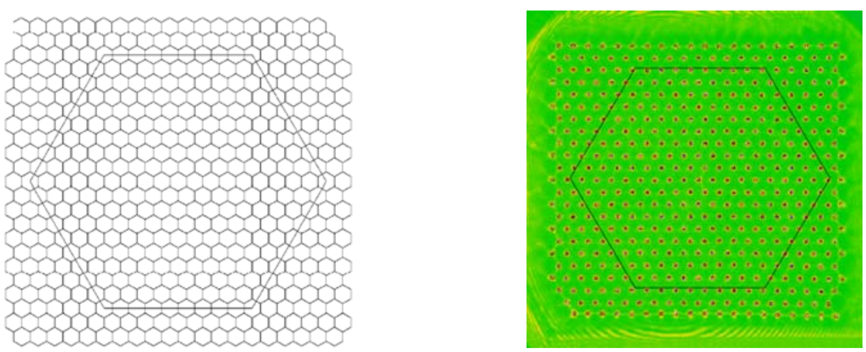

Figure 1: The UFS lenslet array, left hand image, and the UFS Shack Hartman reference spots, right hand image. The outline of a single segment is shown in each image for reference.

Typically the Keck UFS analysis reports only the lowest order Zernike terms. For type I segments, the inner 6 segments that are partially obscured by the secondary mirror, the first 15 Zernike polynomials (excluding piston) are fit to the wavefront measurements. The other 30 segments are fit with the first 45 Zernike polynomials (excluding piston). A wavefront represented by only a small number of Zernike polynomials would tend to be smoother that the actual wavefront that an AO system would be required to correct. A further limitation of the standard UFS wavefront analysis is that it does not include the seven central wavefront slope measurements [1] in its analysis. This omission tends to smooth over the “dimple” at the center of each segment [2]. This dimple is the result of print through from the radial support post at the center of each segment. In order to avoid these limitations, we decided to perform our own reconstruction of the segment figures from the raw UFS slope measurement. We used an iterative method using Fourier transforms originally developed by the Roddiers [3]. Section 2 details the general features of the algorithm. Section 3 gives modifications that are unique to the implementation at Keck used in this report. Section 4 shows some sample segment figures reconstructed with this algorithm.

2. A Fourier Domain Wavefront Reconstruction Algorithm

The problem of estimating a wavefront from slope data has a long history in adaptive optics. Least-squares algorithms are generally used to solve the problem numerically. The underlying wavefront is represented by a set of fitting functions of some sort; these can be either Zernike polynomials or localized actuator influence functions. For this study, we adapted an iterative algorithm based on the Fast Fourier Transform (FFT), originally developed by the Roddiers [3]. This algorithm does not require the use of fitting or basis functions and a further advantage is that the domain of the wavefront reconstruction can have an arbitrary shape.

Hermann [4] (among others) was able to show that the wavefront reconstruction from slope measurements is equivalent to solving Poisson's equation with Neumann boundary conditions. If the wavefront phase function is denoted $\phi(x,y)$ and its gradient is denoted $\boldsymbol{g}=(g_x,g_y)$, the wavefront reconstruction from wavefront slope measurements is equivalent to solution of the following partial differential equation,

$$\nabla^2\phi(x,y) = \nabla\cdot\boldsymbol{g}(x,y)\,. \qquad (1)$$

The basis of the Fourier algorithm is that the Laplacian operator in the spatial domain *(x,y)* transforms into a multiplication in the Fourier domain *(u,v)*,

$$\nabla^2 = \frac{\partial^2}{\partial x^2} + \frac{\partial^2}{\partial y^2} \xrightarrow{FT} u^2 + v^2\,. \qquad (2)$$

If one calculates the Fourier transform of the Laplacian of the wavefront phase, $\nabla^2\phi(x,y)$, divides the result by u^2+v^2, and then applies the inverse Fourier transform, one can recover the underlying wavefront, $\phi(x,y)$. This is the basis for the standard method using Fourier transforms to solve differential equations.

This simple method would work for any function that has no boundary or periodic boundary conditions. In general, the Laplacian of the wavefront, $\phi(x,y)$, will be multiplied by a bounded optical pupil function. The Fourier transform of the Laplacian of the wavefront will be convolved with the Fourier transform of the pupil function. As a result, the simple method outlined above for the solution of Poisson's equation will not hold in the case of a bounded domain. In order to satisfy boundary conditions, Fourier transform methods are generally restricted to square or rectangular shaped boundaries. The method of the Roddiers uses a Grechberg-Saxton algorithm to iteratively solve Poisson's equation on an arbitrary boundary.

The algorithm is outlined in flowchart form in Figure 2. The inputs to the algorithm are two rectangular arrays of numbers that are the wavefront slopes inside the pupil and zero outside. An FFT algorithm is used to calculate the Fourier transform of the input arrays which are now functions of *u* and *v*. The Fourier transform of the x slope is multiplied by u, and that of the y slope is multiplied by v. Both arrays are added, and the result is divided by u^2+v^2 everywhere except at the origin where the ratio is undetermined. Since we seek the solution which has zero mean, we set value of the function to zero at the origin. The resulting function, $\Phi(u,v)$, is the Fourier transform of the wavefront $\phi(x,y)$ in equation 1. Next, one takes the inverse Fourier transform. The resulting wavefront estimate extends outside the boundaries of the pupil. However, only the part of the wavefront inside the boundary is used as the first wavefront estimate. Next step is to take the x and y derivative of the estimate. The results will be different than the original input data. The rms difference between the two sets of wavefront slopes is a measure of the current error in the wavefront reconstruction. The Gerchberg-Saxton algorithm consists of putting the original slope data back into the estimated arrays where measurements have been made and keeping the extrapolated signal outside the pupil. This process is iterated until error is smaller than an assigned level, then the next wavefront estimate is computed and the iterations are stopped.

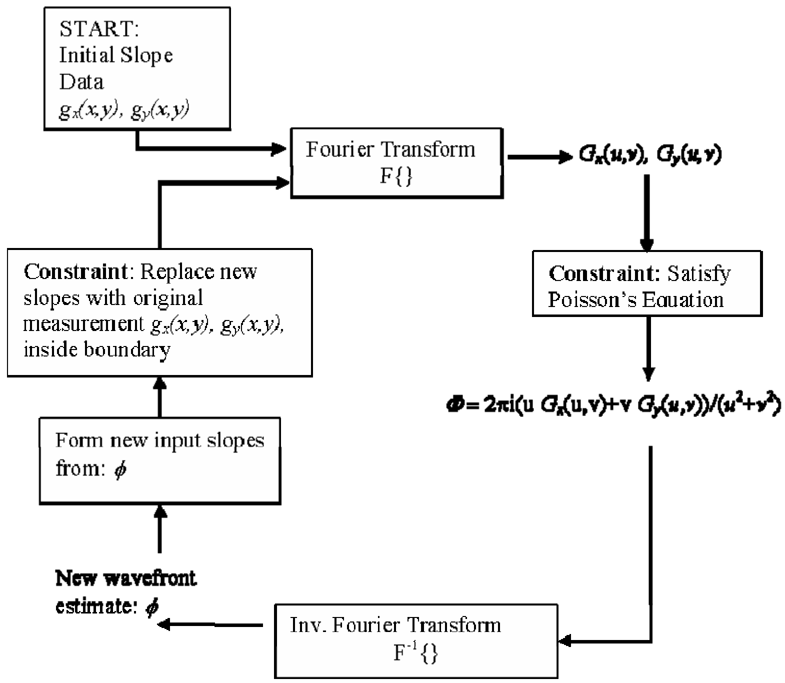

Figure 2: A flow chart that outlines the reconstruction of wavefront phase from wavefront slope data using the method of the Roddiers. The algorithm is based on a modified Gerchberg-Saxton algorithm.

3. Keck Modifications

Although the Roddiers algorithm is very general, some modifications were made for use with the UFS data. As discussed in section 2, the algorithm is able to work on hexagonal domains. However the algorithm still requires slope measurements structured as two dimensional rectangular arrays in order to use the numerical FFT algorithms that were available as part of libraries within the Interactive Data Language (IDL). As shown in Figure 1, the UFS subapertures are arranged in a close packed hexagonal array. The x and y slopes were individually interpolated to a rectangle grid with a spacing that was half the smallest spacing in the hexagonal UFS array. The IDL interpolation algorithm supported irregularly spaced input data.

The majority (24) of the segments in the Keck telescope are unobstructed hexagons, see Figure 3 left most image. The inner 6 segments are partially obstructed by the secondary mirror baffling. For these segments, the hexagonal boundary was truncated on the edge obscured by the secondary, see Figure 3 right hand image. Secondary supports or 'spiders' cut across the diagonal of 6 segments in the middle of the primary, see Figure 3 center image. For these segments, the wavefront slopes were interpolated across the gap using the same IDL interpolation algorithm used on unobstructed segments; it is able to account for gaps in the data. The resulting wavefront maps had no detectable artifacts resulting from the missing slope data.

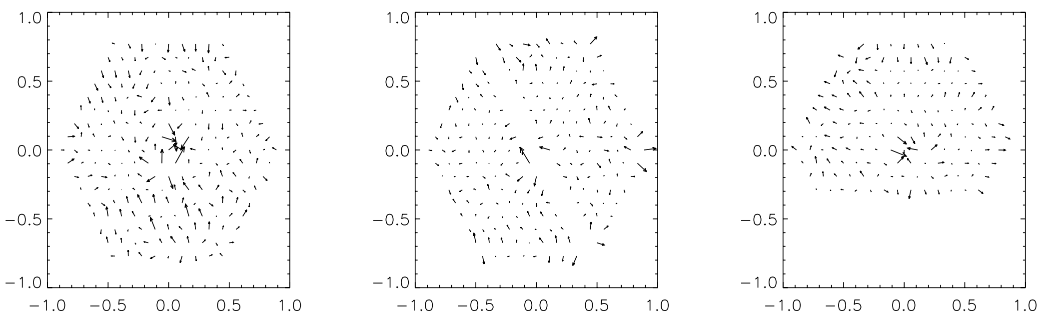

Figure 3: The UFS slope data is represented as 217 arrows in the above plot. Data for each of the three types of segment boundaries shown above can be handled by the algorithm. These are from left to right: full hexagonal segments, slope data obscured by the secondary support struts, and third segments that are obscured by the secondary mirror baffling.

This modified algorithm was used to produce wavefront maps for inclusion into an adaptive optics simulation. These maps were saved as FITS files for later use. For the purposes of the simulation, the full segment wavefront was produced even in the case of the 6 segments that are 30% obscured by the secondary. The algorithm will extrapolate a smooth solution over the obscured region in this case. However, there is no reason to think that this solution is any more accurate in the extrapolated region than other wavefront reconstruction methods when extrapolated over a domain with no input slope data. In the AO simulation, a secondary obscuration was added so that only the visible part of the segment was actually used in the simulation.

4. Sample Segment Wavefront Maps

An example of the wavefront reconstruction of a segment is shown in Figure 4. The images compare the wavefront of segment 4 on Keck II with the warping harness unloaded and after warping in June 2005. Segment 4 unloaded (left image in Figure 4) 907 nm rms and after warping (right image in Figure 4) 113 nm rms. Warping removes lowest order wavefront errors. The same color map was used on both images.

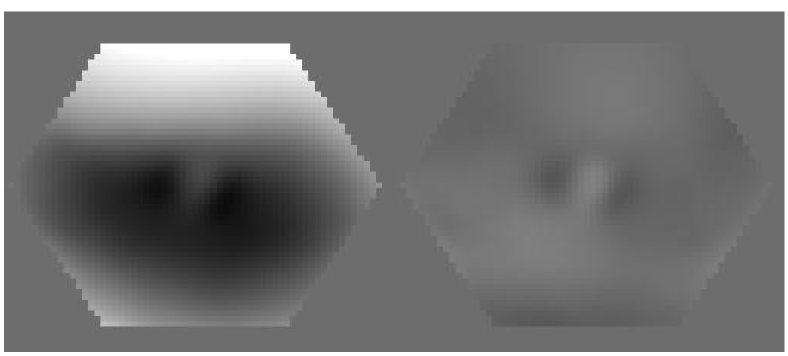

Figure 4: The effects of warping on segment number 4 (PCS numbering convention). The image on the left shows the segment wavefront before warping and the image on the right shows the same segment after warping.

Although segment 4 is about 30% obscured by the secondary the reconstructed wavefront is displayed for the full segment. Next we compare extreme cases of segment figures on Keck II after the segment exchange in June 2005. The images in Figure 5 compare segment number 35 to segment number 4. Segment 35 has an error of 41nm rms and segment 4 has an error of 113 nm rms. The wavefront errors are before correction by an AO system and are the same magnitude as the wavefront error reported for these segments from the standard UFS reduction.

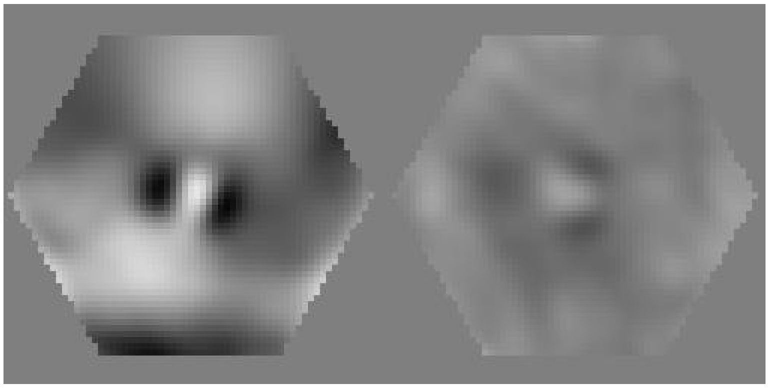

Figure 5: The image on the left shows two extreme cases of segment figures on Keck II after segment warping. The color map is the same for both images.

References

1. G. Chanan and C. Ohara, "Super Ultra fine screen analysis", unpublished report available at: http://sirius.ps.uci.edu/~cohara/sufs.html, page 2 footnotes at bottom.
2. M. Troy, "personal communication", October 2005. After this work was completed, Mitch Troy mentioned that the segment dimples may sometimes cause the seven inner spots to cross over each other, resulting in one spot being confused for its neighbor. The UFS slope algorithm assumes that the nearest Hartmann spot is the correct one for that supaperture. Therefore, the results in this KAON should be taken as lower limits to the actual wavefront that may exist around each radial support post.
3. F. Roddier and C. Roddier, "Wavefront reconstruction using iterative Fourier transforms", Applied Optics, 30, 1325-1327, (1991).
4. J. Hermann, "Least-squares wave front errors of minimum norm", JOSA, 70, 28-35, (1980).